Swelling and growth of polymers, membranes, and sponges

Jack F. Douglas
National Institute of Standards and Technology, Polymers Division, Gaithersburg, Maryland 20899
(Received 18 January 1996)

Polymers can be formed into a wide range of structures depending on the monomer chemistry and the kinetic conditions of growth. A general model of polymers having higher-order connectivity is introduced that reduces to flexible linear polymers, membranes, and sponges as special cases. This ''Wiener sheet'' model, which extends the conventional Wiener path model of linear polymers, is argued to describe various classes of branched polymers, as well as different types of interacting random surfaces. For example, lattice animals and percolation clusters are considered to be perforated sheets whose large-scale dimensions are described by the Wiener sheet model with excluded volume interactions. To within the approximations of the model calculations, the properties of the Wiener sheet ''membrane'' are consistent with this correspondence. The influence of the excluded volume and the kinetics of growth of membrane and sponge structures are treated at a Flory-level approximation, although the Wiener sheet model should admit to a renormalization-group treatment as in the case of linear polymers. Predictions of the self-interacting Wiener sheet model are contrasted with an alternative and complementary random surface model introduced by Nelson and co-workers and are compared with recent simulations and experiment. [S1063-651X(96)00509-0]

PACS number(s): 36.20.Ey, 05.90.+m, 05.40.+j, 82.35.+t

I. INTRODUCTION

Polymers of a networklike structure can be synthesized by polymerizing multifunctional monomers and sheetlike polymers (''membranes'') can be made by polymerizing surface adsorbed monomers [1] or bilayers [2]. Random surface polymers can also be obtained by cleaving layers from crystalline materials [3], such as graphite oxide, and similar sheetlike polymers are believed to naturally arise in certain glassy materials [4]. Membranelike and networklike polymers are also commonly found in biological systems such as cell membranes [5]. Consequently, there is significant motivation for the study of polymers having higher-order chain connectivity. As in the special case of linear chain polymers, the study of mutual and self-excluded volume interactions, hydrodynamic interactions, surface interactions, and the influence of rigidity and the topological form of random surfaces on the properties of materials containing these structures provides a basic field of study. Random sheet models have many other physical applications, which are reviewed by Fröhlich [6] and Nelson [7].

There are evidently a large number of network structures that are possible through the variation of kinetic, chemical, and spatial constraints in the polymerization process. Idealized models are useful in obtaining insights into these branched structures. In the present work we consider a natural generalization of the Wiener path model of linear polymers to describe polymers that are sheetlike or networklike in their connectivity.

A random surface model introduced by Kantor, Kardar, and Nelson [8] (denoted the KKN model) has recently stimulated much analytical and numerical work on polymers of sheetlike connectivity. However, this is not the only generalization of the Wiener path model of polymers. The ''Wiener sheet'' or ''Brownian sheet'' [9,10] model of random surfaces, which has been well studied in the mathematical literature, is also considered as a possible model of random surface polymers. The present exploratory paper indicates some of the exactly known properties of the Wiener sheet and provides a Flory-level description of the influence of excluded volume interactions on these sheetlike structures. Adsorption of sheets onto surfaces and some selected hydrodynamic properties are also considered briefly. Analytic results obtained for the Wiener sheet and KKN random surface models calculations are compared with Monte Carlo simulation (see Fig. 1) and recent experiments on sheetlike

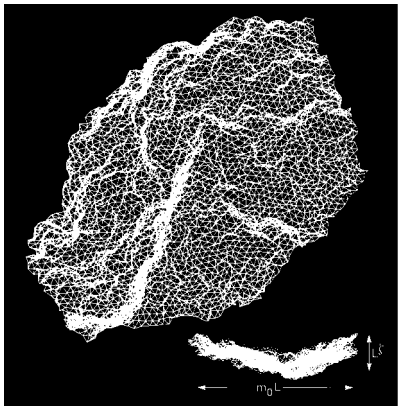

FIG. 1. Tethered self-avoiding random surface [11(d)]. This representative configuration, obtained by molecular-dynamics simulation [11(d)], corresponds to 4219 particles connected by tethers depicted as bonds in the figure. The particles interact with a hard-core repulsion, but are not shown. L denotes the characteristic dimension of the surface in the coordinates of the manifold and m_0 is a nonuniversal constant (see also Fig. 3).

polymers.

Section II provides some background information on the origin and application of random sheet models. The KKN model [8] is briefly reviewed as a point of reference in the discussion of the Wiener sheet model [9,10]. Many of the properties deduced from the Wiener sheet model are rather different from those indicated for the KKN model, although both models are intended to model similar physical systems. Significant discrepancies [11] between the analytic calculations of the KKN model and molecular-dynamics calculations of ''tethered sheet'' polymers have been found and a primary motivation of the present work is to investigate whether the Wiener sheet model [9,10] can more faithfully describe simulated and physical membrane structures [11]. Excluded volume interactions are incorporated into the Wiener sheet model and the radius of gyration exponents ν for swollen Wiener sheets and for θ-point Wiener sheets are calculated at a Flory-level approximation. These calculations indicate unanticipated relations between interacting Wiener sheets (membranes) and branched polymers in good solvents and between percolation clusters and membranes in θ solvents. Networklike polymers of fractal connectivity [12,13] are also considered within the Wiener sheet model. Consideration of network polymers having a three-dimensional topological connectivity indicates an additional ''sponge'' polymer universality class that should be relevant to describing self-avoiding random surfaces having a foamlike structure. The collapse transition, surface adsorption, and dilute solution hydrodynamic properties of membranes are briefly sketched to stimulate further comparisons with experiment. Section III considers the swelling of flexible sheets and sponges due to electrostatic interactions and the kinetic growth of these structures.

II. RANDOM SHEET MODELS

The recent theoretical interest in random surfaces first arose in the context of high-energy physics [14]. Random surfaces arise naturally in field theories that have been proposed to describe the internal structure of subatomic particles. When viewed on a fine level (high energy) it is no longer appropriate to consider such elementary particles as being structureless pointlike particles that sweep out filamentary paths analogous to polymer chain configurations in their shape irregularity. Rather, admitting the spatial extent of the particles leads to a picture in which finite particles sweep out complex volume elements in space-time. From the standpoint of geometry, these ''extended objects'' have much in common with polymer membranes and ordinary polymers at high concentrations. This analogy has stimulated interest in polymeric random surfaces.

The mathematical and the physics literature describing random surfaces is quite extensive and good review articles representing a variety of points of view are available [6,7,15]. The random surface models considered so far come in two primary classes defined in terms of an increase in chain mass with the average radius of the structure. In the absence of interaction one class of ''ideal'' (no excluded volume) random surfaces have a radius of gyration R_g that increases only as the square root of the logarithm of the molecular weight M [16]. The other general class of random surfaces has a R_g that scales as $R_g \sim M^{1/4}$ in the absence of excluded volume interactions [9,11,17]. The scaling of the second class of random surfaces is conspicuously similar to ideal (no excluded volume) branched polymers [18] and numerical evidence and theoretical arguments indicate that certain classes of random surfaces (self-avoiding plaquette surfaces) belong to the branched polymer (''lattice animal'') universality class [19,20], even when the excluded volume is incorporated into these models. Both of these classes of random surface models [$R_g^2 \sim \ln(M)$, $R_g \sim M^{1/4}$] are natural generalizations of the Wiener path model of linear polymers (see below) [21]. Boulatov *et al.* [17(d)] have considered a more general random surface model that exhibits a crossover between these random surface models involving an ''intrinsic curvature'' parameter α. The KKN and Wiener sheet models can thus be expected to be *complementary* models of random surfaces.

A. The KKN random surface model

Kantor, Kardar, and Nelson introduced an analytic theory of flexible surfaces of fixed connectivity embedded in a d-dimensional space [8]. Extensive theoretical and numerical literature was stimulated by this publication [11,22]. Excitement was initially generated by a Flory-level description [8] of the excluded volume in this random surface model, which indicated agreement with preliminary numerical calculations [8]. Later simulations established a significant deviations between the analytic KKN model calculations and the simulations, however [11]. The KKN model and some results based on this model are summarized below for comparison with the Wiener sheet model. Part of the motivation of considering the Wiener sheet model is to determine if this model gives a more accurate description of the universal properties of the simulated and real random surfaces with excluded volume interactions.

The KKN model is a natural generalization of the Wiener path model of polymer chains [21]. A point on the surface of the sheetlike polymer is specified by a position vector $\mathbf{R}(\boldsymbol{\tau})$. The coordinate variable, however, is itself a vector in the manifold coordinates $\boldsymbol{\tau}=(\tau_1,\tau_2,\ldots,\tau_{d_m})$, where d_m is the manifold dimension. For a linear polymer $\boldsymbol{\tau}$ reduces to just a scalar variable τ specifying the contour coordinate along the chain. The sheet is specified by the $\mathbf{R}(\boldsymbol{\tau})$ spatial coordinates embedded in a d-dimensional space and the manifold Ω coordinates. L is a characteristic scale of the manifold such as the side length of a square manifold sheet and is measured in the Euclidean metric of the sheet coordinates. Configurational properties of KKN sheets are calculated by averaging over all surfaces with respect to the Boltzmann weight $\exp(-H/k_BT)$, where the Hamiltonian equals [8]

$$H(\mathbf{R}(\boldsymbol{\tau}))/k_BT = H_0(\mathbf{R}(\boldsymbol{\tau})) + (\beta_z/2)\int_\Omega d\boldsymbol{\tau}\int_\Omega d\boldsymbol{\tau}' \times \delta(\mathbf{R}(\boldsymbol{\tau})-\mathbf{R}(\boldsymbol{\tau}')), \tag{2.1a}$$

$$H_0(\mathbf{R}(\boldsymbol{\tau})) = \tfrac{1}{2}\int_\Omega d\boldsymbol{\tau}\left|\nabla_{\boldsymbol{\tau}}(\mathbf{R}(\boldsymbol{\tau}))\right|^2, \tag{2.1b}$$

where β_2 is the binary cluster integral. This model reduces to the ''two-parameter model'' (or ''Edward's model'') of the

polymer excluded volume [21,23] for manifolds of dimension $d_m=1$ (ordinary linear polymer chains). However, this is not a *unique* extension of the linear polymer model to describe random surfaces (see below).

The Flory-type calculation for the radius of gyration exponent for the KKN random surface model is a generalization of the linear polymer calculation. There is an elastic term R^2/L^{2-d_m} from H_0 in Eq. (2.1b) and an excluded volume interaction contribution $\beta_2 L^{2d_m}/R^d$. Summing these terms, taking the derivative with respect to R, and setting the result equal to zero gives the result of Kantor, Kardar, and Nelson for the average sheet radius R [8],

$$\overline{R}\sim L^{\hat{\nu}}, \quad \hat{\nu}=(d_m+2)/(d+2). \tag{2.2a}$$

The total mass M of the sheet scales with its size L as $M\sim L^{d_m}$ so that the swollen sheet size scales with mass as [8]

$$\overline{R}\sim M^{\nu}, \quad \nu=(d_m+2)/d_m(d+2). \tag{2.2b}$$

A caret is put over the exponent $\hat{\nu}$ in Eq. (2.2a) to distinguish it from the related mass scaling exponent ν in Eq. (2.2b). This model predicts that sheets without excluded volume are extraordinarily compact for $d_m>1$,

$$\overline{R_0^2}\sim L^{2-d_m}, \quad d_m<2, \tag{2.2c}$$

reducing to a logarithmic variation $\overline{R_0^2}\sim \ln L$ as d_m approaches $d_m\to 2-$. These networks are ''collapsed'' or ''localized'' for $d_m>2$ since R_0^2 is *then independent of* L. Simulations of tethered random surfaces in the *absence* of excluded volume interactions have verified the logarithmic scaling [11(d)] in Eq. (2.2c) for $d_m=2$.

The scaling of random surface dimensions according to Eq. (2.2c) was implicit in earlier work on Gaussian chain networks by James and Guth [24]. Ronca and Allegra [25] have shown a relation between the radius of gyration of the Gaussian chain network model of James and Guth and the resistivity of networks. The characteristic logarithmic variation of R_0^2 also describes the resistance between two points separated by a large distance L in a plane net of resistors [25(c)]. The KKN model then has many potential applications, apart from the description of certain model random surfaces.

It has been argued [13,26] that the manifold dimension d_m in the KKN random surface model can be *formally* replaced by the ''spectral dimension'' $d_s\to d_m$, which governs the rate of random-walk exploration on the manifold defining the chain connectivity. Levinson [12] has presented numerical evidence supporting this proposal. However, exact calculations [27] for the Wiener sheet, discussed below, (rigorously) indicate a different definition of the ''effective topological dimension'' of Wiener random sheets so that the identification of $d_s\to d_m$ should be taken with some caution. This problem deserves further investigation.

Initial Monte Carlo data and table top experiments with crumpled foil balls indicated [8] an exponent $\hat{\nu}$ ($d_m=2$, $d=3$) consistent with Eq. (2.2a); $\hat{\nu}\approx 0.8$. More recent and larger-scale molecular-dynamics simulations (see Fig. 1) have established that $\hat{\nu}$ is near unity in three dimensions [11] and that Eq. (2.2a) is not an accurate approximation. (Because the scaling relation $\overline{R}\sim L$ is reminiscent of the scaling of a plane sheet these random surfaces are referred to as being ''flat.'' Specific realizations of these surfaces are actually rather crumpled looking, so the term should not be taken too literally.) Because of the conflict between their simulation data and the KKN random surface model, Grest and Murat [28] attempted to ''crumple'' (decrease $\hat{\nu}$) in their simulated surfaces by punching holes at random positions in them and letting the structures relax. Surprisingly, this decimation process gave rise to *no detectable change* in the scaling properties of the random surface until the holes reached the percolation threshold [28,29], whereupon the whole structure disintegrated. The significance of this important observation is discussed in Sec. II B.

Difficulties are also encountered in analytic calculations based on the Hamiltonian in Eq. (2.1) [26]. Examination of the scaling of the m-body excluded volume interaction for this model in a fashion parallel to linear polymers reveals that the m-body interactions scale with molecular weight as

$$z_m(\mathrm{KKN})\sim M^{\phi_m}, \quad \phi_m(\mathrm{KKN})=m, \tag{2.3}$$

where $\ln(M)$ terms are neglected. Formally, the relevance of m-body interactions *increases* with the order of the m-body interaction. The physical appropriateness of including only binary excluded volume interactions is certainly a question. Even neglecting the somewhat arbitrary truncation of excluded volume interactions at the binary interaction level, a formal calculation of the resulting model ($d_m=2$) reveals a perturbation theory having an ''infinite critical dimension'' and a reference model having an ''infinite fractal dimension'' [16]. Application of the ϵ-expansion method is then out of the question unless the manifold dimension is formally taken as variable, $d_m<2$ [26]. Apart from these technical difficulties, the main problem with the model at the present stage of development is the observed inconsistency between model predictions [such as Eq. (2.2)] and the simulation data mentioned above.

Goulian [30] recently made an alternative ''Gaussian approximation'' estimate of $\hat{\nu}$ for swollen sheets starting from Eq. (2.1), which led to better agreement with numerical estimates of $\hat{\nu}$ as a function of dimension d [31]. At a Flory-level description this calculation amounts to taking the excluded volume contribution $\beta_2 L^{2d_m}/R^d$ in the Hamiltonian, defined in Eq. (2.1), on the order of a constant and *neglecting* the elastic contribution to the free energy. This argument gives

$$\overline{R}\sim L^{\hat{\nu}}\sim M^{\nu}, \quad \hat{\nu}=2d_m/d, \quad \nu=2/d, \tag{2.4}$$

which for a two-dimensional ($d_m=2$) sheet reduces to the case considered explicitly by Goulian [30]. The linear polymer estimate ($d_m=1$) corresponding to Eq. (2.4) corresponds to the classical Reiss–Des Cloizeaux estimate [32] $\nu=2/d$, and in this case the predicted value of ν is known to be inaccurate. Although Goulian's calculation seems to gives an improved estimate for $\hat{\nu}$ for random surfaces ($d_m=2$) over a range of dimensions [31] in comparison with the KKN Flory-theory calculation [8], this argument still does not lead to accurate estimates of $\hat{\nu}$ for the swollen sheet in $d=3$. This calculation does suggest, however, that the shortcoming of

the KKN model in describing tethered surfaces is associated with the elastic contribution to the free energy.

B. Wiener sheet model of random surfaces

There is another model of random surfaces that is a natural generalization of the Wiener path model of linear polymers. The Wiener (or Brownian) sheet model [9,10] is described by a surface represented by position vectors $\mathbf{R}(\boldsymbol{\tau})$ defined as in the KKN model. The Wiener sheet corresponds to an independent random process where the individual position components of $\mathbf{R}(\boldsymbol{\tau})$ obey a covariance relation in the $\boldsymbol{\tau}$ coordinate similar to Brownian motion [9,10]. (This is a defining characteristic of these random surfaces and an understanding of how this type of surface emerges as the continuum limit of discrete microscopic models of random surfaces is an outstanding problem.) The Wiener sheet model has been studied extensively over the past 30 years [see, e.g., [9(d)]] and we therefore limit the discussion to some of the well established properties of this model. In this initial study Flory-type calculations are also developed to make a qualitative check of the model in relation to simulation and experimental data.

In the absence of self-excluded volume interactions the fractal (Hausdorff) dimension d_f of the Wiener sheet has rigorously been proven to equal [9(a),10(a)]

$$d_f = \min(2d_m, d). \tag{2.5}$$

The minimum relation occurs since the Hausdorff dimension *cannot* exceed the spatial dimension d. The relation Eq. (2.5) corresponds to the average radius R of the Wiener sheet scaling as

$$\overline{R_0} \sim L^{\nu_0} \sim M^{\nu_0}, \quad \nu_0 = \tfrac{1}{2}, \quad \nu_0 = 1/2d_m, \tag{2.6a}$$

where the zero subscript denotes the absence of excluded volume interactions. The average radius of a membrane ($d_m=2$) or linear polymer ($d_m=1$) in the absence of excluded volume interactions scales as

$$\overline{R_0} \sim \begin{cases} M^{1/2} & \text{(linear polymer, noninteracting)} \quad (2.6b) \\ M^{1/4} & \text{(membrane polymer, nonintearacting).} \quad (2.6c) \end{cases}$$

The random-walk result Eq. (2.6b) is familiar and the membrane model result Eq. (2.6c) was suggested by Parisi [17(a)] for noninteracting random surfaces ($d_m=2$). We also recognize that the scaling of the surface radius with mass corresponds to the Flory-Stockmayer theory [18] of ''branched polymers'' and this connection is discussed further below.

Montford [27] considered generalizations of the Wiener random sheet whose network connectivity is defined as a fractal set. His results show that if the mass elements of the sheet are positioned on a manifold of fractal dimension d_{fm} then the fractal (Hausdorff) dimension d_f of the resulting Wiener sheet in space (rigorously) equals

$$d_{fm} = 2d_m, \tag{2.7}$$

where d_f is less than or equal to d. This result means that the manifold dimension d_m should be replaced by the fractal (Hausdorff) dimension d_{fm} rather than a spectral dimension in the calculation of ν in the case of the Wiener sheet. Equation (2.7) is important in our discussion below of random sheets of irregular connectivity. (Below the fractal dimension d_f will refer to the mass scaling exponent [e.g., $d_f=2d_m$ in Eq. (2.6a)] rather than the Hausdorff dimension so that the min terminology in Eq. (2.5) is avoided.)

The incorporation of excluded volume interactions into the Wiener sheet model is a simple matter in a Flory-level approximation. Formally, the interaction terms are the *same* as in the KKN model. The distribution function between two points on the surface is a *Gaussian function* in the Wiener sheet model [9(a), 9(d)], as in the case of linear polymers, and we thus have the elastic contribution R^2/L and a binary excluded volume contribution $\beta_2 L^{2d_m}/R^d$ as in the KKN surface model calculation summarized in Sec. II A. Adding these contributions and minimizing in the usual fashion gives the Flory-type estimate of ν for the Wiener sheet

$$\overline{R} \sim L^{\hat{\nu}} \sim M^{\nu}, \quad \hat{\nu} = (2d_m+1)/(d+2),$$
$$\nu = (2d_m+1)/d_m(d+2). \tag{2.8}$$

Taking $d_m=2$ and $d=3$ we find $\hat{\nu}=1$ and $\nu=1/2$, which is compatible with numerical simulations on simulated swollen tethered random surfaces [11]. It then seems plausible that the local rigidity (''intrinsic curvature'' [17(d)]) of the random surface is strongly perturbed by excluded volume interactions so that the Wiener sheet provides a better reference model for the swelling of random surfaces than the KKN model. This presumption is hard to prove, but it is possible to explore some of the many implications of this hypothesis. Moreover, the problem of the swelling of Wiener sheets should have independent interest.

The simple noninteracting Wiener sheet model applies for d high enough that the probability of self-intersection becomes negligible [9(d)]. It is well known that the ideal Wiener path model describes long swollen linear polymers for dimensions greater than 4. Recent direct enumeration calculations of ν for self-avoiding walks in Fig. 2 illustrate this variation. Simple dimensional analysis based on the Wiener sheet model and consideration of the binary interaction in Eq. (2.1) allows the formal deduction of the critical dimension for the self-interacting Wiener sheet. The dimensionless m-body interactions z_m scale with random surface mass M as

$$z_m \sim \beta_m L^{D_m}, \quad D_m = 2d_m m - (m-1)d, \tag{2.9}$$

corresponding to a scaling of z_m with mass

$$z_m \sim \beta_m M^{\phi_m}, \quad \phi_m = m - (m-1)d/2d_m. \tag{2.10}$$

This is a direct generalization of the scaling of the dimensionless excluded volume interaction for linear polymers. From Eq. (2.10) we see that $d=8$ is a critical dimension for binary ($m=2$) excluded volume interactions and $d=6$ is a critical dimension for ternary interactions ($m=3$) in a membrane ($d_m=2$). In accord with these scaling results for the Wiener sheet ($d_m=2$) rigorous calculations [9(d)] indicate that the probability of nontrivial Wiener sheet intersection vanishes above $d=8$ and the scaling exponent D_m defines the fractal (Hausdorff) dimension of the m-body self-intersection set [33]. Parisi [17(a)] previously suggested that the lower critical dimension [see Eq. (2.5)] for a class of random surfaces was $d=4$ [corresponding to $\phi_m=1$ in Eq. (2.10)] and

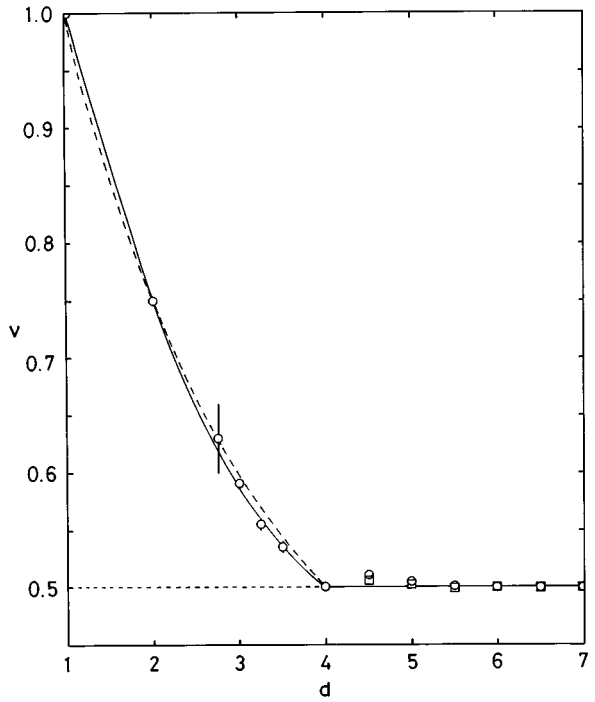

FIG. 2. Estimation of the SAW exponent ν obtained by direct enumeration and ratio method extrapolation [69]. The solid line represents an analytic interpolation formula that is closely approximated (dashed line) by the Flory-theory estimate $\nu=3/(d+2)$. See Ref. [69] for an explanation of the lattice data.

$d=8$ was an upper critical dimension for binary excluded volume interactions and discussed some of the important physical implications of these geometrical relations. These conjectures exactly accord with the known properties of the Wiener sheet ($d_m=2$).

Flory-type estimates of the θ-point exponent ν_θ for self-interacting Wiener sheets are also possible. First, it is naively assumed that *only* ternary interactions are relevant in determining ν_θ. Adding the ternary interaction L^{3d_m}/R^{2d} to the elastic term R^2/L and minimizing gives, in the tenary approximation, for $d\leqslant 3d_m$,

$$\overline{R}_\theta\sim L^{\hat{\nu}_\theta}\sim M^{\nu_\theta},\quad \hat{\nu}_\theta=(3d_m+1)/2(d+1),$$
$$\nu_\theta=(3d_m+1)/2d_m(d+1). \tag{2.11}$$

The linear polymer case $\nu_\theta\approx 2/(d+1)$ is known to be rather inaccurate in $d=2$ [34], however, so that quantitative agreement with Eq. (2.11) with experimental and simulation data cannot be expected (see below).

A basic problem with Flory-type estimate of ν_θ is the retention of only ternary interactions under circumstances where higher-order interaction are also relevant. Isaacson and Lubensky [35] introduced an alternative modeling of ν for concentrated polymer solutions where higher-order interactions are also important. They suggest modeling the binary interaction by a ''renormalized'' interaction $\beta_2(L^{2d_m}/R^d)\,L^{-\alpha}$ in the case $d_m=1$. The $L^{-\alpha}$ term is intended to reflect the ''screening'' of the binary interactions within a chain by the other chains in solution. This idea can also be adapted to estimate the θ-point exponent ν_θ of membranes where the $L^{-\alpha}$ term is assumed to reflect the influence of ternary and higher-order interactions. The magnitude of α can be *fixed* by noting that the critical dimension for ternary interactions equals $d_{c,3}=3d_m$ from Eq. (2.10) and higher-order interactions are irrelevant for $d>3d_m$. Taking $d_m=2$ (membranes) for specificity, we should then have ideal behavior ($R_0\sim L^{1/2}\sim M^{1/4}$) for $d\leqslant 6$ dimensions. With this constraint in mind we add the interaction term $\beta_2(L^{2d_m}/R^d)L^{-\alpha}$ to R^2/L and minimize to obtain

$$\overline{R}_\theta\sim L^{\hat{\nu}_\theta},\quad \hat{\nu}_\theta=(4+1-\alpha)/(d+2). \tag{2.12}$$

The exponent α must be 1 at $d=6$ to recover the classical exponent $\hat{\nu}_0=\frac{1}{2}$ and following Isaacson and Lubensky [35] in the context of their discussion of the swelling of ''gelation clusters'' we take $\alpha=1$ generally. This approximation gives an approximation for $\hat{\nu}_\theta$ for a membrane,

$$\hat{\nu}_\theta=\begin{cases}4/(d+2), & d<3d_m=6,\quad d_m=2 \qquad (2.13a)\\ \frac{1}{2}, & d\geqslant 6. \qquad (2.13b)\end{cases}$$

Equation (2.13a) corresponds (fortuitously) to the KKN random surface exponent $\hat{\nu}(d_m=2)$ in Eq. (2.2a), aside from the restriction $d<6$ in Eq. (2.13a).

The Flory-theory estimates of the self-avoiding and θ-point Weiner sheets reveal an unanticipated relation between the Weiner sheet ($d_m=2$), branched polymers (lattice animals), and percolation clusters. Expressing the average radius of a self-avoiding Weiner sheet in terms of the mass of the sheet indicates

$$\overline{R}(d_m=2)\sim M^{\nu},\quad \nu=\begin{cases}5/[2(d+2)], & d<4d_m=8\\ \frac{1}{4}, & d>8.\end{cases} \tag{2.14a}$$

(ν is related generally to the manifold dimension d_m and the fractal dimension of the surface d_f as $\hat{\nu}=d_m/d_f=d_m\nu$.) The critical dimension of branched polymers for binary excluded volume interactions is well known [18] to be $d_c(m=2)=8$ and the exponent $\nu=5/[2(d+2)]$, $d\leqslant 8$ is exactly the Isaacson-Lubensky Flory-theory estimate [18] for ν (lattice animal). The critical dimension of percolation clusters is $d=6$ [36] and ν_θ in Eq. (2.13a) also describes the mass scaling of percolation clusters

$$\overline{R}_\theta\sim M^{\nu_\theta},\quad \nu_\theta=\begin{cases}2/(d+2), & d\leqslant 6\\ \frac{1}{4}, & d\geqslant 6\end{cases} \tag{2.14b}$$

within a Fory-level approximation. Exact formal calculations [34(a),34(b)] indicate that ν_θ in $d=2$ for linear polymers is the mass scaling exponent of ''percolation hulls'' in $d=2$, indicating another relation between the θ-point scaling of Wiener sheets [$\nu_\theta(d_m=1,\ d=2)=\frac{4}{7}$] and percolation theory. The hulls of percolation clusters in $d=3$ have a fractal dimension closely corresponding to $1/\nu_\theta$ in Eq. (2.14b) (see below) so there is some evidence that this geometric connection extends to higher d (see below).

A direct relation between branched polymers (lattice animals) and self-avoiding random surfaces is strikingly shown in the simulations of Grest and Murat [28] (see Fig. 3). They find that the scaling of the membrane dimensions with mass

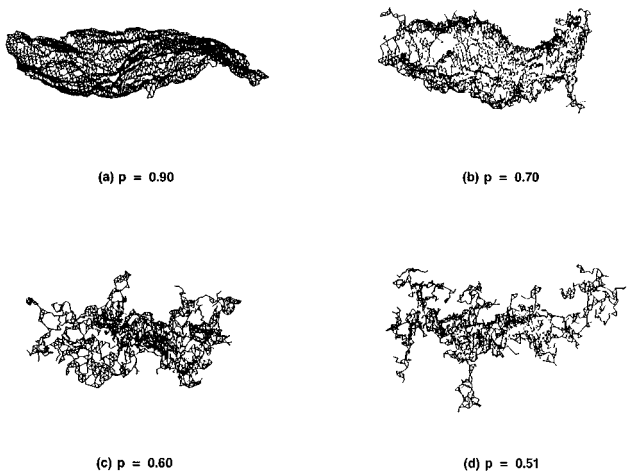

FIG. 3. Self-avoiding tethered surfaces with randomly cut bonds [28]. $1-p$ denotes the concentration of bonds that have been cut. The molecular-dynamics study of Grest and Murat [28] shows that the exponent ν is *unaffected* by the bond cutting to within numerical uncertainty so that branched polymers ($p \approx 1/2$) seem to correspond to a perforated swollen ''membrane.'' This connection is also found in Flory-type calculations for ν using the Wiener sheet random surface model (see text).

is *independent of hole concentration* to within numerical uncertainty up to the hole percolation threshold p_c. Near p_c the decimated membrane is clearly a branched polymer and this numerical study strongly suggests that self-avoiding membranes belong to the lattice animal universality class (Grest and Murat did not make this point in their numerical study). These decimated sheet simulations and this point of view make the connection between the Wiener sheet estimate for ν in Eq. (2.14) and previously known results for branched polymers and percolation clusters almost obvious.

Figure 4 compares Eq. (2.14a) to estimates [38] of the exponent ν for swollen branched polymers (lattice animals) in various spatial dimensions d. As is well known, the agreement is rather good, as in the case of linear polymers (see Fig. 2). Further, de Gennes [39] has developed a model of percolation clusters as branched polymers subject to intercluster screening of excluded volume interactions. These connections between branched polymers and self-avoiding membranes suggest that the exponent ν, describing the mean size of percolation clusters, *equals* the θ-point exponent ν_θ for self-interacting membranes. Another possibility is that $1/\nu_\theta$ for the membrane equals the fractal dimension of the hull of percolation clusters, which would be a natural extension of the linear chain results [34(a),34(b)] and consistent with recent numerical data for the percolation hull dimension $d_f \approx 2.5$ [37]. Finally, we mention that Eq. (2.11) corresponds to Daoud and Joanny's estimate [40] of ν_θ for branched polymers. The Wiener sheet model then offers the prospect of a unified model of linear and branched polymers.

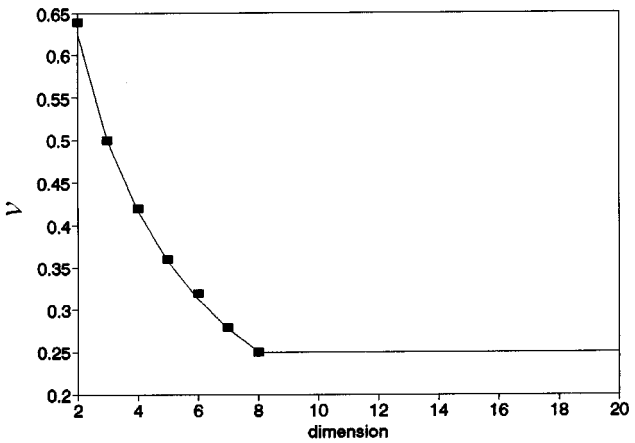

FIG. 4. Exponent ν for a self-avoiding Wiener sheet ($d_m=2$), a membrane. The filled squares correspond to numerical estimates of ν for branched polymers (''lattice animals'') [17,18]. The solid line is the Flory-theory prediction for the dimensional variation of ν, which is the *same* as for the swollen Wiener sheet.

Some exact results are known for lattice animals and percolation clusters and in other cases precise numerical estimates are available (see Fig. 4). These results allow for a quantitative comparison between the properties of random sheets and branched polymers. The exponent ν for lattice animals in $d=3$ and 4 equals $\nu=\frac{1}{2}$ and $\frac{5}{12}$, respectively [41]. These values agree with the Flory-theory value of ν for membranes in Eq. (2.14a) and these estimates are conjectured to be *exact* for self-avoiding membranes as well ($d_m=2$), so that $\hat{\nu}(d=3)=1$ and $\hat{\nu}(d=4)=\frac{5}{6}$. (Grest's numerical estimate [31] of $\hat{\nu}$ is somewhat higher in four dimensions $\hat{\nu} \approx 0.91$, although further work on larger systems would be helpful in assessing the accuracy of this value.) Estimating ν_θ as the reciprocal fractal dimension of percolation clusters [42] yields $\hat{\nu}_\theta(d=2)=\frac{48}{91}$ and $\hat{\nu}_\theta(d=6)=\frac{1}{4}$ and numerical calculation [43] gives $\hat{\nu}_\theta(d=3)=0.402$. Agreement with the Flory estimate from Eq. (2.14b), $\hat{\nu}_\theta(d=3)=\frac{4}{10}$, is again rather good. We next mention some relevant experimental data for branched polymers that should be consistent with the random surface data by the arguments above. Bouchaud *et al.* [44] observe $1/\nu=1.98\pm0.03$ for diluted branched polymers (gelation clusters) in good accord with the expectations of lattice animals and Adam *et al.* [45] obtain $1/\nu=2.5\pm0.09$ for undiluted branched polymers. These results are consistent with expectations for branched polymers or Wiener membranes in good and θ solvents, respectively. Recent experiments [46] on branched dextran polymers in the θ solvent water gave $1/\nu_\theta \approx 2.5$. Finally, we note recent molecular-dynamics simulations of flexible tethered random sheets that indicate that $d_f \approx 2.4$ at the θ point [22]. The observed excluded volume dependence of branched polymers is similar to simulations of the swelling of tethered sheets and with the Flory-theory estimates of the swelling of membrane polymers (see Sec. II E).

Sheetlike surfaces have also been obtained by exfoliating graphite with strong oxidizing agents [3]. Light-scattering measurements on these surfaces indicate $1/\nu=2.4\pm0.1$ and $1/\nu \approx 3$, dependent on solvent conditions. These preliminary exponent estimates are consistent with ν_θ in Eq. (2.14) and the value of ν expected for collapsed surfaces (see Sec. II E). It is unclear, however, whether these measurements are made under equilibrium conditions.

C. ''Sponge'' polymers

Another important class of Wiener sheets corresponds to a polymer having a three-dimensional lattice net (e.g., cubic lattice) connectivity. Allowing such a structure to relax into a disordered configuration gives rise to a sponge polymer. [In

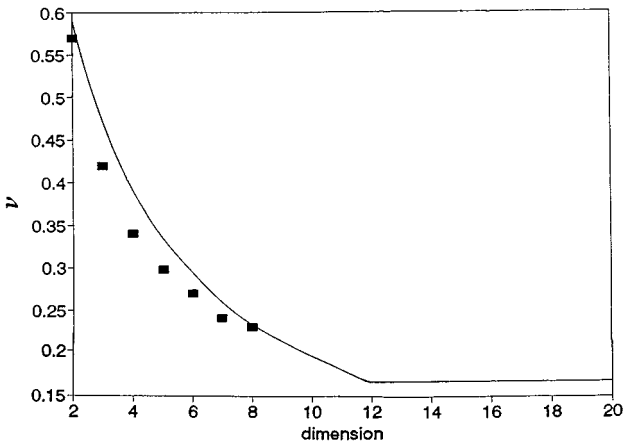

FIG. 5. Exponent ν for a swollen ''sponge.'' The solid line denotes the Flory-theory estimate of ν for the Wiener sheet ($d_m=3$) from Eq. (2.15b). The filled squares correspond to values for ''bushy'' branched polymers grown by a sequential kinetic growth process [47]. These ν data correspond to the reciprocal fractal dimension values $1/d_f$ reported by Alexanderowicz [47]. Branched polymers grown under continuous growth conditions led to exponents close to those for lattice animals (see Fig. 4).

KKN model calculations such generalized polymers ($d_m=3$) are sometimes referred to as ''gels,'' but this term is avoided because it is often employed with a rather different meaning in polymer science.] Simulation studies have not been made for these sponge polymers, but the expected results for these structures can be estimated based on the Wiener sheet model ($d_m=3$). Related numerical and experimental observations are also examined in light of these theoretical results.

From Eq. (2.10) the critical dimension for binary excluded volume interactions ($m=2$, $d_m=3$) is $d=12$ and the θ-point critical dimension for ternary excluded volume interactions for the sponge is $d=9$. The average radius $\overline{R}$ of the swollen sponge in the Flory approximation then scales as, for $d_m=3$,

$$\overline{R}\sim L^{\hat{\nu}}\sim M^{\nu}, \quad \hat{\nu}=7/(d+2), \quad \nu=7/[3(d+2)], \quad d<12 \tag{2.15a}$$

and the θ-point exponents equal

$$\overline{R}\sim L^{\hat{\nu}_\theta}\sim M^{\nu_\theta}, \quad \hat{\nu}_\theta=11/[2(d+2)],$$
$$\nu_\theta=11/[6(d+2)], \quad d<9. \tag{2.15b}$$

Above $d=12$ the mass exponent ν is equal to $\frac{1}{6}$ so that sponge polymers tend to be rather compact. The variation of ν for the swollen sponge [Eq. (2.15)] is indicated in Fig. 5.

The discussion of Sec. II B suggests that representations of the sponge universality class of self-avoiding random surface's might correspond to a class of branched polymers. With this possibility in mind we examine the simulations of branched polymers by Alexandrowicz [47], since this work emphasizes the existence of more than one branched polymer universality class, depending on growth conditions. In particular, ''bushy'' branched polymers grown in sequential generations (reminiscent of ''dendrimers'' [48]) gave different ν values than branched polymers grown under equilibrium conditions. The exponent ν for these stepwise generated polymers tended to be more compact than regular branched polymers. In Fig. 4 the numerical values of $1/d_f$ for the stepwise generated branched polymers is compared with Eq. (2.15b). Alexandrowicz [47] estimates the reciprocal fractal dimension in the limit of high dimensionality as roughly $1/d_f\approx 0.22$ and he found somewhat smaller values of the effective ν exponent, $\nu\approx(0.1, 0.13)$, describing the scaling of the average size of these polymers. These exponent estimates are compared to the exact sponge value $\nu=\frac{1}{6}$ for $d>12$. The simulation values of ν for ordinary branched polymers, which are believed to be in the lattice animal universality class, are presented in Fig. 5 for comparison. Evidently, these two classes of branched polymers are rather distinct, as indicated by Alexandrowicz [47]. The stepwise growth and continuous growth polymers (also considered by Alexandrowicz) seem to conform well to the self-avoiding sponge ($d_m=3$) and membrane ($d_m=2$) model predictions, respectively. This comparison, of course, is rather heuristic.

We next consider some other branched polymer structures grown under nonequilibrium conditions in a further qualitative comparison to the sponge model. Data for the silica colloid aggregates indicate $1/\nu=2.12\pm0.05$, where $1/\nu$ is reported as the aggregate fractal dimension by Schaefer *et al.* [49]. The corresponding self-avoiding sponge prediction is $1/\nu=\frac{15}{7}\approx 2.14$. Experiments on zinc electrodeposit aggregates in $d=2$ [50] indicate $1/\nu=1.66\pm0.03$, which is compared with the sponge model estimate in $d=2$, $1/\nu=\frac{12}{7}\approx 1.71$, from Eq. (2.15a). These favorable comparisons suggest that it might be worth looking more carefully at this phenomenon based on the sponge model. The sponge model may also have significant biological relevance. Protein molecules can often be idealized as random surfaces and recent experiments have shown a surprising degree of universality for the fractal dimensions of many proteins that are found to lie in the narrow range $d_f\equiv 1/\nu=2.14\pm0.04$ [51]. This range is also consistent with the swollen sponge model prediction $d_f\approx 2.14$ from Eq. (2.15b).

There is another class of branched polymers that is interesting to compare with the self-avoiding sponge model. Wessel and Ball [52] consider the diffusion-limited aggregation (DLA) model [53], generalized to allow for aggregated particles to disaggregate so that an ''equilibrium structure'' is obtained. They argue and provide numerical evidence that the disaggregation model of DLA generated polymers is in the lattice animal universality class. An estimate of the kinetic growth of sponges is developed in Sec. III.

D. Random plaquette surfaces

Another random surface model involves placing square ''plaquettes'' on a lattice edge to edge where no overlaps are allowed [19] (the elementary plaquettes can also be cubes). Numerical calculations for this generalization of self-avoiding lattice walks indicate that the the geometrical properties of these random surfaces again closely correspond to those of branched polymers [19]. For example, a recent Monte Carlo estimate of ν for this kind of random surface gives [19(c)]

$$\nu(d=2)=0.506\pm0.005 \tag{2.16}$$

and similar but less precise estimates have been obtained by direct enumeration [19(e)]. This exponent estimate is restricted to self-avoiding plaquette surfaces having no loops

(''handles''). This kind of constraint is similar to the ''light branching'' constraint in linear polymers [55] (light branching corresponds to the formation of a ring, star, or comb chain topology and this low degree of branching does not change the linear chain self-avoiding walk exponent ν).

Self-avoiding random plaquette surfaces (SARPS) with an arbitrary number of loops more resemble a spongelike structure and a change of universality class from branched polymer (lattice animals) to another universality class seems plausible when the number of loops is large. Banavar, Maritan, and Stella [54] have previously argued for this possibility, although they argue that the resulting highly branched polymers are compact ($d_f=3$). The situation is quite similar to the linear to branched polymer (lattice animal) crossover obtained by increasing the number of chain cross links. It seems very likely that the SARPS with a high degree of looping correspond to the sponge universality class [this conjecture remains to be tested by a recently developed numerical algorithms developed at NIST to simulate SARPS with a high degree of looping [19(e)]. The proposed relation between sponge polymers and SARPS with a large number of loops indicates that such SARPS should exhibit a significantly different critical behavior (contrast ν values in Figs. 4 and 5).

Maritan, Seno, and Stella [56a] recently indicated a class of SARPS corresponding to the hulls of Ising model clusters. The fractal dimension of these Ising clusters is estimated to satisfy the bound $1.88 \leqslant 1/\nu \leqslant 2.16$ for $d=3$, which is again consistent (roughly) with the Flory-theory estimates of the sponge exponents [56b]. It would be interesting if future simulations of this class of SARPS and Ising critical clusters confirmed a relation to the sponge model. The directly observable clusters [57] in critical fluid mixtures certainly certainly have a spongelike appearance and the fractal dimension of these critical clusters ($d_f \approx 2.8 \pm 0.01$) is consistent with the sponge θ-point estimate ($d_f \approx 2.72$) from Eq. (2.15b), appropriate for a high concentration of critical clusters where screening of the excluded volume interactions should arise.

Random plaquette surfaces with a high propensity to form loops should rather resemble an open cell foamlike structure and this model has great potential for the modeling spongy materials such a microemulsions and the disordered phase of block copolymer fluids. Measurements on certain amphiphilic molecule materials such as lipids and soap molecules often reveal a bicontinuous latticelike structure that can ''melt'' into a disordered spongelike phase [58(a)] and this type of order-disorder transition is also commonly encountered in block copolymer materials [58(b)]. It remains to be seen whether the Wiener sponge model is applicable in the quantitative description of any of these physical systems, but the model appears promising for these material science applications.

E. Collapse of a ''membrane''

The presence of attractive self-interactions in the Wiener sheet causes a decrease in the average polymer dimensions as in linear polymers. This effect is so important that it deserves a separate discussion. For the self-interacting membrane ($d_m=2$) Eqs. (2.11) and (2.14b) imply

$$\overline{R}(T \gg \theta) \sim L^{\hat{\nu}} \sim M^{\nu}, \quad \hat{\nu}=5/(d+2), \quad \nu=5/[2(d+2)], \quad d<8 \tag{2.17a}$$

$$\overline{R}_{\theta}(T \approx \theta) \sim L^{\hat{\nu}_{\theta}} \sim M^{\nu_{\theta}}, \quad \hat{\nu}_{\theta}=4/(d+2), \quad \nu_{\theta}=2/(d+2), \quad d<6 \tag{2.17b}$$

$$\overline{R}(T \ll \theta) \sim L^{\hat{\nu}_c} \sim M^{\nu_c}, \quad \hat{\nu}_c=2/d, \quad \nu_c=1/d, \tag{2.17c}$$

where the collapsed sheet exponent $\nu_c=1/d$ is estimated by assuming that the collapsed surfaces achieves a uniform segment density for sufficiently large attractive interactions. This same assumption is conventional in discussions of linear polymer collapse. It would be interesting to examine the θ-point in these surfaces more carefully to determine the magnitude of ν_{θ} in comparison with Eq. (2.14b). Note that Eq. (2.17) implies that a θ-point membrane is crumpled ($\hat{\nu}_{\theta}<1$). This effect was recently observed in simulations [22], as mentioned above. Experimental estimates [3] of ν for dissolved graphite sheets are also in accord with Eqs. (2.17b) and (2.17c), which is consistent with the measurements being made in a poor or marginal solvent. Osmotic pressure measurements could confirm this possibility.

III. WIENER SHEETS WITH SURFACE AND HYDRODYNAMIC INTERACTIONS

Treatment of surface and hydrodynamic interactions in the Wiener sheet is a direct extension of the linear polymer problem. For example, we may consider the interaction Hamiltonian [59] for a random sheet interacting with a Euclidean surface (point, line plane, etc.) of dimension $d_{\parallel}$,

$$H_I=\beta_s \int_{\Omega} d\boldsymbol{\tau}\, \delta(\mathbf{R}_{\perp}(\boldsymbol{\tau})), \tag{3.1}$$

where β_s is the coupling constant between the random surface and the Euclidean surface. The vector $\mathbf{R}_{\perp}(\boldsymbol{\tau})$ in Eq. (3.1) is the component of the sheet coordinate $\mathbf{R}(\boldsymbol{\tau})$, which is normal to the Euclidean surface of dimension $d_{\parallel}$, $d_{\perp}+d_{\parallel}=d$. Dimensional analysis based on Eq. (3.1) indicates that the dimensionless surface interaction scales z_s as, for $0<\phi_s \leqslant 1$,

$$z_s \sim \beta_s M^{\phi_s} \sim \beta_s L^{D_s},$$

$$\phi_s=1-(d-d_{\parallel})/2d_m,$$

$$D_s=d_m-(d-d_{\parallel})/2, \tag{3.2}$$

where D_s is the fractal dimension of the intersection between the membrane and the Euclidean plane (see [27] for a rigorous discussion of D_s for the case $d_{\parallel}=0$). The perturbative calculation of surface interacting sheet properties is formally similar to those for linear polymers near an interacting boundary [59,60].

Adsorption of a sheet onto a surface should give rise to an extensive change in free energy $\Delta F \sim M$ as in the case of linear polymers. Consistency of the free-energy scaling with Eq. (3.2) implies that the free energy of a random surface adsorbed on a Euclidean surface scales as [60]

$$\Delta F \sim |z_s|^{1/\phi_s}, \quad \Delta F/M \sim |\beta_s|^{1/\phi_s}. \tag{3.3}$$

Thus the order of the surface adsorption phase transition of a membrane ($d_m=2$) onto a surface of dimension $d_\parallel$ ($d_\parallel=0$, point; $d_\parallel=1$, line; $d_\parallel=2$, plane; etc.) equals $1/\phi_s$ [60]. For a plane surface ($d_\parallel=2$) in $d=3$ dimensions the membrane interaction exponent equals $\phi_s=\frac{3}{4}$ and the order of the transition is $\frac{4}{3}$ (see Ref. [60] for a discussion of fractional order transitions). The linear chain polymer exhibits a second-order transition onto the plane surface so the membrane should exhibit a sharper transition than its linear chain topology counterpart. The inclusion of excluded volume interactions into the sheet could alter this conclusion, however.

At a rough configurational preaveraging level approximation [61,62] we can deduce the scaling for Wiener sheet hydrodynamic interactions and the scaling behavior of some basic hydrodynamic solution properties. The preaveraged Oseen tensor scales like the Coulomb potential ($|\mathbf{R}|^{-(d-2)}$) and from dimensional analysis the scaling of the dimensionless hydrodynamic interaction h with chain mass M is readily deduced for an ideal Wiener sheet

$$h\sim(\zeta/\eta_s)M^{\phi_H},\quad \phi_H=1-(d-2)/2d_m, \tag{3.4}$$

where ζ is the monomer friction. For an arbitrary fractal $2d_m$ in Eq. (3.4) is replaced by the sheet fractal dimension. The scaling of the dimensionless hydrodynamic interaction h is not so simple if the preaveraging approximation is not employed, but Eq. (3.4) should remain qualitatively correct. The translational friction f_T of a Wiener sheet, within a generalization of the Kirkwood-Riseman theory [61], should be reasonably approximated by [62]

$$f_T=n\zeta/[1+A(\zeta/\eta_s)M^{\phi_H}], \tag{3.5a}$$

$$f_T\sim M^{(d-2)/2d_m},\quad h\to\infty, \tag{3.5b}$$

where A is a constant on the order of unity. Note that the critical dimension d_{cH} of the translational friction f_T of an ideal Wiener sheet equals

$$2d_m+2=d_{cH} \tag{3.6a}$$

and for a swollen ''fractal object'' of dimension d_f, Eqs. (3.4), (3.5b), and (3.6a) become for strong hydrodynamic interaction,

$$f_T\sim M^{(d-2)/d_f},\ \ d_f+2=d_{cH},\ \ \phi_H=1-(d-2)/d_f \tag{3.6b}$$

For rodlike chains ($d_m=1$) $d=3$ is critical (ϕ_H formally vanishes) and $d=4$ is critical for random coil shaped polymers. In contrast, for swollen membranes ($d_m=2$) and flat plates $d=4$ is critical [62]. The translational friction f_T generically has a logarithmic variation on the mass M at the critical dimension, as in the case of rodlike polymers in $d=3$. Above the critical dimension f_T is proportional to the polymer, membrane, or sponge mass M. If these objects are taken to have a position volume.

The intrinsic viscosity of a slender body scales [64] as $[\eta]\sim f_T R_G^2/M$ and a swollen membrane is presumed to swell similarly. The friction scales as $f_T\sim M^{(d-2)\nu}$ [numerical calculation of f_T for membranes and ''sponges'' is feasible [[63(b)]] so that $[\eta]$ for a swollen membrane should have the molecular weight dependence

$$[\eta]\sim M^{1/2},\quad d=3, \tag{3.7a}$$

where we have used $\nu\ (d=3;d_m=2)=\frac{1}{2}$ from Eq. (2.14a). (The intrinsic viscosity of a flat plate, swollen membrane, or ideal linear polymer chain all have the same molecular weight dependence since these objects have the same fractal dimension.) Experiments [1(b)] on sheetlike polymers formed by polymerizing surface-adsorbed poly(methyl methacrylate) indicate a rough variation $[\eta]\sim M^{1/2}$ in accord with Eq. (3.7a). This agreement may be fortuitous, however, and more generally scaling arguments indicate that $[\eta]$ scales as

$$[\eta]\sim M^{(3d-4)/2(d+2)},\quad 2\leqslant d<8 \tag{3.7b}$$

$$[\eta]_\theta\sim M^{(d-2)/(d+2)},\quad 2\leqslant d<6, \tag{3.7c}$$

which shows that the viscosity exponent is rather dependent on solvent quality (i.e., temperature). The intrinsic viscosity exponent should be much smaller ($\frac{1}{5}$) in a θ solvent and independent of molecular weight in a very poor solvent where the membrane is in a compact form [63(c)].

This section provides a brief description of surface and hydrodynamically interacting membranes based on the Wiener surface model. Direct calculation of Wiener sheet properties follow the same general patterns as linear polymers, but the calculations become technically more complicated.

IV. SWELLING OF FLEXIBLE SHEETS AND SPONGES DUE TO ELECTROSTATIC INTERACTIONS AND THE GROWTH OF MEMBRANES AND SHEETS

Naturally occurring membranes often ionize in an aqueous environment. At high salt concentrations these bare charges are largely screened by counterions and the problem of swelling reduces in large measure to an ordinary excluded volume interactions. At lower salt concentrations the ions within the sheets strongly interact and consequently modify the sheet configuration. Suppose for simplicity that the charges are distributed continuously over the surface. The question is then how a membrane or sponge swells under these circumstances. Within a primitive Flory-type modeling this question is readily answered, although it should be appreciated that this type of modeling is very crude.

The generalization of the Flory theory to describe the swelling due to electrostatic repulsion follows from a consideration of the symmetries of the δ-function pseudo-potential for the excluded volume interaction and for the Coulomb potential under rescaling of lengths. The δ function obeys the scaling relation $\delta(\lambda\mathbf{R})=\lambda^d\delta(\mathbf{R})$ and the Coulomb potential scales as $V(\lambda\mathbf{R})=\lambda^{d-2}V(\mathbf{R})$. The interaction term for a binary interaction is of the general form

$$\beta_\delta L^{2d_m}/R^s, \tag{4.1}$$

where β_δ is a coupling constant (excluded volume, electrostatic, etc.) and s is the homogeneity index of the potential. Notice that the only place that dimensionality comes into the Flory-type calculation is through the constant s, characterizing the symmetry of the interaction potential under rescaling. In the electrostatic interaction problem $s=d-2$ and in the excluded volume problem $s=d$ so that the problems are related by a simple *dimensional shift* $d\to d-2$. Taking

$d \to d-2$ in the excluded volume result Eq. (2.11) gives an estimate of ν for random surfaces with unscreened electrostatic interactions

$$\nu=[(2d_m+1)/d]/d_m; \tag{4.2}$$

In $d \leqslant 3$ we see that linear charged polymers are highly swollen $\nu=1$ since ν cannot exceed 1. A charged membrane ($d_m=2$) should likewise be ''flat'' for $d \leqslant 3$.

Another general factor affecting the exponent ν is the order of the excluded volume interaction. It is useful to consider, for example, a ''one-body'' version of the excluded volume interaction, the ''true self-avoiding surface.'' The excluded volume interaction in this case is built up as the surface grows so that only a factor L^{d_m} arises in the polymer self-interaction term. The potential has homogeneity index $s=d$ as in ordinary excluded volume, so that total self-interaction term equals $\beta_\delta L^{d_m}/R^d$. Minimizing the free energy in the usual way gives

$$\nu=(d_m+1)/d_m(d+2), \quad d<d_{cT}=2d_m, \tag{4.3}$$

where d_{cT} is the critical dimension for this type of ''local'' excluded volume interaction. Simulations agree very well with this prediction for linear chains ($d_m=1$) [65] and this result perhaps has some relevance to the kinetic growth of membranes and sponges since the critical dimensions are then $d=4$ and 6, respectively, the lower critical dimensions of the Wiener sheet. The true self-avoiding surface is meant to describe the growth of membranes ($d_m=2$) and sponges ($d_m=3$) under conditions where the surrounding medium has a saturated concentration of the monomer material needed for growth. The volume exclusion effect actually develops in time as the structure grows. Another extreme case corresponds to the situation where the concentration of monomer for growth is more limited so that the growth is governed by the rate of diffusion to the aggregate. This is the kind of growth process that inspired the classic diffusion-limited aggregation model [53].

In Sec. II C an approximate relation between a particular kinetic growth model of branched polymers and the sponge ($d_m=3$) Wiener surfaces was suggested and we next treat the growth of sponges where diffusion-limited nature of the growth is considered. The interaction term develops kinetically in time, as in the true self-avoiding surface model, so that we have a L^{d_m} factor for the sponge ($d_m=3$) self-interaction. However, the potential governing the growth is nonlocal because the aggregate induces a depletion in the concentration of monomer in its surroundings. From Smoluchowski theory [66] the concentration field to which the aggregate growth is responding is the Coulomb potential $|\mathbf{R}|^{-(d-2)}$, which governs the probability of a random walk launched from large distance from the growing sponge to hit the sponge [63(b)]. Thus we take the interaction term $\beta_\delta L^{d_m}/R^{d-2}$ and add it to the elastic term and minimize as usual to obtain

$$\overline{R} \sim M^{4/3d} \tag{4.4}$$

for the sponge growing under diffusion-limited conditions. This rather heuristic estimate ν agrees qualitatively with the rough numerical estimates of ν for DLA approximated by

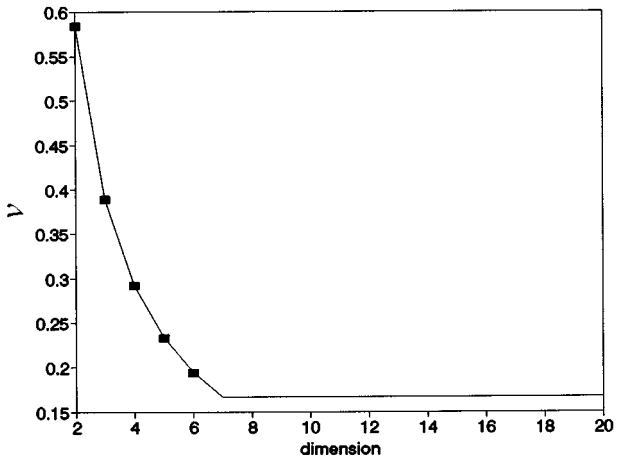

FIG. 6. Estimate of ν for diffusion-limited growth of a sponge. The filled squares denote simulation data for ν of diffusion-limited aggregates obtained by Meakin [67] (see the text for an explanation of this comparison and assumptions associated with this estimate).

$\nu(\mathrm{DLA})=6/5d$ [67] (see below for an improved estimate). It should be mentioned that in this idealized model of diffusion-limited growth model there is a critical dimension ($d_c=2d_m+2$), while it is is widely believed that DLA growth does not have a finite upper critical dimension as in the KKN model [68]. This feature is not captured by the Wiener sheet model. The intrinsic curvature (see Ref. [17(d)]) may well become diminished in high dimension so that the KNN model becomes a better model of the random surfaces and the critical dimension then becomes infinite.

The calculation of ν in Eq. (4.4) does not take into account screening effects and this effect is responsible for much of subtlety of the DLA growth process. Again following Lubensky and Isaacson [18], we can consider the extreme limit of screening corresponding to an extra factor $L^{-\alpha}$ in the interaction term, where $\alpha=1$. A value of $\alpha=1$ exactly cancels the L^{-1} term in the elastic term when we consider the free-energy minimization. This limiting case of screening ($\alpha=1$) implies $\nu=1/d$ or the growth of a compact sponge. For the sake of illustration we take α to have the intermediate value $\frac{1}{2}$ to obtain $\nu=7/6d$. This estimate of ν for the diffusion limited growth of a sponge (with the *ad hoc* choice of the screening parameter $\alpha=\frac{1}{2}$) agrees well with DLA simulation data [67] and a comparison with DLA data is shown in Fig. 6.

It is evident that by varying the conditions controlling the deposition of monomer to a growing aggregate a wide range of growth patterns in sponges and membranes should be possible. Such processes are important in the natural development of fractal structures in the physical world. The fractal dimension of the structure and other geometrical information of these clusters preserve a memory of the kinetic conditions under which the structure was formed. Basically these structures are ''fossils'' of the kinetic growth process.

V. CONCLUSION

There are numerous physical processes that can be modeled by random-walk paths. In condensed matter these processes include equilibrium phase transitions (liquid vapor,

liquid-liquid phase separation magnetic phase transitions, etc.). The random-walk model provides a basic model of polymer chains in the bulk and in solution. The existence of higher-order connectivity in sponge, membrane, or irregular branched polymer configurations requires more general models than Brownian motion for the specification of the large-scale properties of these structures. The Wiener sheet [9,10] generalization of Brownian motion provides an important generalization that should have a wide range of applications beyond the polymer models discussed in the present paper. The challenge is to understand the geometrical properties of these general random surfaces and the relation of their geometrical properties to the many physical processes naturally described by this type of model.

In the present exploratory paper we emphasize the geometrical properties of the Wiener sheet model. Many properties of these surfaces have been established rigorously by mathematicians working in this field over many years [9,10]. The new contribution involves pointing out the relevance of this model to polymer science and the inclusion of excluded volume interactions into this random surface model at the level of Flory theory. The results of these simple model calculations are compared with recent molecular-dynamics simulations of random surfaces [11,12] and experiments [3] on real random surfaces. The simulations suggest a remarkable ''universality'' and provocative relations between branched polymers and random surfaces. For example, the exponent ν for flexible tethered sheets with excluded volume is very close to that for self-avoiding random plaquette surfaces [19]. Grest and Murat [28] and Plischke and Fourcade [29] made the interesting observation that adding holes at random into a tethered random sheet apparently has *no apparent effect* on the critical exponent ν. The picture of branched polymers that emerges is quite simple. Increasing branching in linear polymers leads to a series of transitions in the effective topological dimension from linear to sheetlike ($d_m=2$) to spongelike ($d_m=3$) polymeric forms. From this point of view branched polymers are perforated sheets or networks that are incompletely connected, as beautifully illustrated in the simulations of Grest and Murat. It is also notable that the ideal Wiener sheet model leads to ideal rubber elasticity and the model is much more realistic than single-chain models' network elasticity.

The Wiener sheet model is very convenient for the calculation of random surface and branched polymer properties since the whole machinery of the renormalization group and self-consistent field theory can be readily generalized from the case of linear polymers [21]. Further work is needed to understand how the Wiener sheet model emerges as a continuum limit of microscopic random surface models.

ACKNOWLEDGMENTS

Many thanks are given to Farid Abraham and Gary Grest for providing Figs. 1 and 4, respectively. Discussions with Arkady Kholodenko of Clemson University are also appreciated.

[1] (a) A. Blumstein, R. Blumstein, and T. H. Vanderspurt, J. Colloid Interface Sci. **31**, 236 (1969); (b) A. Blumstein, J. Herz, V. Sinn, and C. Sadron, C. R. Acad. Sci. **246**, 1856 (1958).

[2] S. L. Regen, J.-S. Shin, J. F. Hainfield, and J. S. Wall, J. Am. Chem. Soc. **106**, 5756 (1984); M. Mutz, D. Bensimon, and M. J. Brienne, Phys. Rev. Lett. **67**, 923 (1991); J. H. Fendler and P. Tundo, Acct. Chem. Res. **17**, 3 (1984).

[3] T. Hwa, E. Kokufuta, and T. Tanaka, Phys. Rev. A **44**, R2235 (1991); X. Wen, C. W. Garland, T. Hwa, M. Kardar, E. Kokufuta, Y. Li, M. Orkisz, and T. Tanaka, Nature **355**, 426 (1992).

[4] M. J. Aziz, N. Nygren, J. F. Hays, and D. Turnbull, J. Appl. Phys. **57**, 2233 (1985). See Ref. [8].

[5] A. Elgsaeter, B. T. Stokke, A. Mikkelsen, and D. Branton, Science **234**, 1217 (1986); C. F. Schmidt, K. Svoboda, N. Lei, I. B. Petsche, L. E. Berman, C. R. Safinya, and G. S. Grest, *ibid.* **259**, 952 (1993).

[6] J. Fröhlich, in *Sitges Conference Statistical Mechanics*, edited by L. Garrido, *Lecture Notes in Physics* Vol. 216 (Springer-Verlag, New York, 1985), p. 31; see also Ref. [15].

[7] D. R. Nelson, in *Statistical Mechanics of Membranes and Surfaces*, edited by D. R. Nelson, T. Piran, and S. Weinberg (World Scientific, Singapore, 1989).

[8] Y. Kantor, M. Kardar, and D. R. Nelson, Phys. Rev. Lett. **57**, 791 (1986); Phys. Rev. A **35**, 3056 (1987); M. Kardar and D. R. Nelson, Phys. Rev. Lett. **58**, 1289 (1987).

[9] (a) L. Yoder, Ann. Prob. **3**, 169 (1975); (b) J. P. Nolan, *ibid.* **16**, 1596 (1988); (c) W. Ehm, Z. Wahr. **56**, 195 (1981); (d) R. Epstein, Ann. Prob. **17**, 538 (1989).

[10] (a) L. T. Tran, Ann. Prob. **7**, 532 (1979); **17**, 538 (1989); Z. Wahr. **37**, 27 (1976); (b) R. J. Adler, *The Geometry of Random Fields* (Wiley, New York, 1981); Ann. Prob. **6**, 509 (1978); (c) S. Orey and W. Pruitt, *ibid.* **1**, 138 (1973); (d) W. S. Kendall, Z. Wahr. **52**, 267 (1980); (e) H. P. McKean, Theor. Prob. Appl. **8**, 335 (1963).

[11] (a) M. Plischke and D. Boal, Phys. Rev. A **38**, 4943 (1988); (b) J. S. Ho and A. Baumgartner, Phys. Rev. Lett. **63**, 1324 (1989); (c) F. F. Abraham, W. E. Rudge, and M. Plischke, *ibid.* **62**, 1757 (1989); (d) F. F. Abraham and D. R. Nelson, Science **249**, 393 (1990); J. Phys. (Paris) **51**, 2653 (1990).

[12] E. Levinson, Phys. Rev. A **43**, 5233 (1991).

[13] M. E. Cates, Phys. Lett. **161B**, 363 (1985).

[14] A. M. Polyakov, *Gauge Theory and Strings* (Harwood Academic, New York, 1982); Nucl. Phys. B **268**, 406 (1986); A. A. Migdal, *ibid.* **189**, 253 (1981); V. A. Kazakov, Phys. Lett. **128B**, 316 (1983); T. Eguchi, Phys. Rev. Lett. **44**, 126 (1980).

[15] J. F. Wheater, J. Phys. A **27**, 3323 (1994).

[16] D. Gross, Phys. Lett. **138B**, 185 (1984). Strickly speaking, the Hausdorff dimension of an object cannot exceed the spatial dimension *d* of the embedding space; *ibid.* B. Duplantier, *ibid.* **141B**, 239 (1984); J. Jurkiewicz and A. Krzywicki, *ibid.* **148B**, 148 (1984); R. L. Renken and J. B. Kogut, Nucl. Phys. B **342**, 753 (1990); A. Billoire, D. J. Gross, and E. Marinari, Phys. Lett. **139B**, 75 (1984).

[17] (a) G. Parisi, Phys. Lett. **81B**, 357 (1979); (b) H. Tasaki and T.

Hara, *ibid*. **112A**, 115 (1985); (c) B. Durhuus, T. Fröhlich, and T. Jonsson, Nucl. Phys. B **257**, 779 (1985); (d) D. V. Boulatov, V. A. Kazakov, I. K. Kostov, and A. A. Migdal, *ibid*. **275**, 641 (1986); (e) A. L. Stella, E. Orlandini, I. Beichl, F. Sullivan, M. C. Tesi, and T. L. Einstein, Phys. Rev. Lett. **69**, 3650 (1992).

[18] B. H. Zimm and W. H. Stockmayer, J. Chem. Phys. **17**, 1301 (1949); T. C. Lubensky and J. Isaacson, Phys. Rev. A **20**, 2130 (1979); J. Phys. (Paris) **42**, 175 (1981); M. Daoud, P. Pincus, W. H. Stockmayer, and T. Witten, Macromolecules **16**, 1833 (1983); D. Dhar, Phys. Rev. Lett. **51**, 853 (1983); B. Derrida and L. De Seze, J. Phys. (Paris) **43**, 475 (1982).

[19] (a) U. Glaus, J. Stat. Phys. **50**, 1141 (1988); (b) U. Glaus and T. L. Einstein, J. Phys. A **20**, L105 (1987); (c) J. O'Connell, F. Sullivan, D. Libes, E. Orlandini, M. C. Tesi, A. L. Stella, and T. L. Einstein, *ibid*. **24**, 4619 (1991); (d) A. Baumgartner and A. Romero, Physica A **187**, 243 (1992); (e) S. Redner, J. Phys. A **18**, L723 (1985).

[20] B. Durhuus, T. Jonsson, and J. Fröhlich, Nucl. Phys. B **240**, 453 (1984).

[21] K. F. Freed, *Renormalization Group Theory of Macromolecules* (Wiley, New York, 1987); J. Des Cloizeaux and G. Jannink, *Polymers in Solution* (Clarendon, Oxford, 1990).

[22] G. S. Grest and I. B. Petsche, Phys. Rev. E **50**, R1737 (1994). This work reviews recent theoretical and numerical studies of self-avoiding membranes.

[23] H. Yamakawa, *Modern Theory of Polymer Solutions* (Harper and Row, New York, 1971).

[24] H. M. James, J. Chem. Phys. **15**, 651 (1947); H. M. James and E. Guth, *ibid*. **15**, 669 (1947).

[25] (a) G. Ronca and G. Allegra, J. Chem. Phys. **63**, 4104 (1975); **65**, 2043 (1976); (b) B. E. Eichinger, Macromolecules **5**, 496 (1972); (c) G. H. Vineyard, J. Math. Phys. **4**, 1191 (1963).

[26] J. A. Aronovitz and T. C. Lubensky, Europhys. Lett. **4**, 395 (1987); B. Duplantier, Phys. Rev. Lett. **58**, 2733 (1987); M. Kardar and D. R. Nelson, Phys. Rev. A **38**, 966 (1988).

[27] T. S. Montford, Ann. Prob. **17**, 1454 (1989).

[28] G. S. Grest and M. Murat, J. Phys. (Paris) **51**, 1415 (1990).

[29] M. Plischke and B. Fourcade, Phys. Rev. A **43**, 2056 (1991).

[30] M. Goulian, J. Phys. (France) II **1**, 1327 (1991).

[31] G. S. Grest, J. Phys. (France) I **1**, 1695 (1991).

[32] H. Reiss, J. Chem. Phys. **47**, 186 (1967); J. Des Cloizeaux, J. Phys. (Paris) **31**, 715 (1970).

[33] C. Xiong, Ind. Univ. Math. J. **43**, 55 (1994); J. Rosen, Ann. Prob. **12**, 108 (1984).

[34] (a) A. Coniglio, N. Jan, I. Majid, and H. E. Stanley, Phys. Rev. B **35**, 3617 (1987); (b) B. Duplantier and H. Saleur, Phys. Rev. Lett. **59**, 539 (1987); **62**, 1368 (1989); (c) J. F. Douglas, B. J. Cherayil, and K. F. Freed, Macromolecules **18**, 2455 (1985).

[35] J. Isaacson and T. C. Lubensky, J. Phys. (Paris) Lett. **41**, 469 (1980).

[36] R. G. Priest and T. C. Lubensky, Phys. Rev. B **13**, 4159 (1976); D. J. Amit, J. Phys. A **9**, 1441 (1976); T. C. Lubensky and J. Isaacson, Phys. Rev. Lett. **41**, 828 (1978).

[37] P. N. Strenski, R. M. Bradley, and J. M. Debierre, Phys. Rev. Lett. **66**, 1330 (1991); R. M. Bradley, Phys. Rev. E **49**, 1909 (1994).

[38] S. Havlin and D. Ben-Avraham, Adv. Phys. **36**, 695 (1987). This work summarizes numerous results related to lattice animals.

[39] P. G. De Gennes, C. R. Acad. Sci. B **291**, 17 (1980).

[40] M. Daoud and J. F. Joanny, J. Phys. (Paris) **42**, 1359 (1981).

[41] G. Parisi and N. Sourlas, Phys. Rev. Lett. **46**, 871 (1981).

[42] D. Stauffer, *Introduction to Pecolation Theory*, 2nd ed. (Taylor and Francis, Philadelphia, 1992); T. Hara and G. Slade, Commun. Math. Phys. **128**, 333 (1990); J. Stat. Phys. **59**, 1469 (1990); J. Adler, Phys. Rev. B **41**, 9183 (1990); D. Stauffer, Phys. Rep. **54**, 3 (1979).

[43] A. Margolina, H. J. Hermann, and D. Stauffer, Phys. Lett. **93A**, 73 (1982).

[44] E. Bouchaud, M. Delsanti, M. Adam, M. Daoud, and D. Durand, J. Phys. (Paris) **47**, 1273 (1986).

[45] M. Adam, M. Delsanti, J. P. Munch, and D. Durand, J. Phys. (Paris) **48**, 1809 (1987).

[46] J. A. Smit, J. A. van Dijk, M. G. Mennen, and M. Daoud, Macromolecules **25**, 3585 (1992).

[47] Z. Alexanderowicz, Phys. Rev. Lett. **54**, 1420 (1985).

[48] P. G. De Gennes and H. Hervet, J. Phys. Lett. **44**, L351 (1983); R. L. Lescanec and M. Muthukamar, Macromolecules **23**, 2280 (1990); D. A. Tomalia, A. M. Naylor, and W. A. Goddard III, Angew Chem. (Int. Ed.) **29**, 138 (1990).

[49] W. Schaefer, J. E. Martin, P. Wiltzius, and D. S. Cannell, Phys. Rev. Lett. **52**, 2371 (1984).

[50] M. Matsushita, M. Sano, Y. Hawakawa, H. Honjo, and Y. Sawada, Phys. Rev. Lett. **53**, 286 (1984).

[51] B. A. Fedorov, B. B. Fedorov, and P. W. Schmidt, J. Chem. Phys. **99**, 4076 (1993); P. Feifer, U. Welz, and H. Wippermann, Chem. Phys. Lett. **113**, 535 (1985).

[52] R. Wessel and R. C. Ball, Phys. Rev. A **45**, R2177 (1992).

[53] (a) T. A. Witten and L. M. Sander, Phys. Rev. Lett. **47**, 1400 (1981); (b) J.-M. Debierre and R. M. Bradley, J. Phys. A **22**, L213 (1989); (c) M. Y. Linn, H. M. Lindsay, D. A. Weitz, R. C. Ball, R. Klein, and P. Meakin, Nature **339**, 360 (1989).

[54] J. R. Banavar, M. Maritan, and A. Stella, Science **252**, 825 (1991).

[55] J. F. Douglas, J. Roovers, and K. F. Freed, Macromolecules **23**, 4168 (1990).

[56] (a) A. Maritan, F. Seno, and A. L. Stella, Phys. Rev. B **44**, 2834 (1991); (b) A. L. Stella, Phys. Rev. E **50**, 3259 (1994).

[57] P. Guenon, F. Perrot, and D. Beysens, Phys. Rev. Lett. **63**, 1152 (1989).

[58] (a) R. Lipowsky, Nature **349**, 475 (1991); (b) F. S. Bates and G. H. Fredrickson, Annu. Rev. Phys. Chem. **41**, 525 (1990).

[59] B. Duplantier, Phys. Rev. Lett. **62**, 2337 (1989).

[60] J. F. Douglas, S. Q. Wang, and K. F. Freed, Macromolecules **19**, 2207 (1986); J. F. Douglas, *ibid*. **22**, 1786 (1989).

[61] J. G. Kirkwood and J. Riseman, J. Chem. Phys. **16**, 565 (1948).

[62] J. F. Douglas, H.-X. Zhou, and J. B. Hubbard, Phys. Rev. E **49**, 5319 (1994).

[63] (a) J. B. Hubbard and J. F. Douglas, Phys. Rev. E **47**, R2983 (1993); (b) J. F. Douglas, H.-X. Zhou, and J. B. Hubbard, *ibid*. **49**, 5319 (1994); (c) J. F. Douglas and G. Garboczi, Adv. Chem. Phys. **91**, 85 (1995).

[64] G. Weill and J. Des Cloizeaux, J. Phys. (Paris) **40**, 99 (1979); J. Douglas and K. F. Freed, Macromolecules **27**, 6088 (1994).

[65] R. Rammal, J. C. Angles d'Auriac, and A. Benoit, J. Phys. A **17**, L9 (1984); L. Pietronero, Phys. Rev. B **27**, 5887 (1983).

[66] M. Smoluchowski, Z. Phys. Chem. **92**, 129 (1917); H. C. Berg and E. M. Purcell, Biophys. J. **20**, 193 (1977); C. Collins and G. E. Kimball, J. Colloid. Sci. **4**, 425 (1949); J. M. Deutch and P. Meakin, J. Chem. Phys. **78**, 2093 (1983).

[67] P. Meakin, Phys. Rev. A **27**, 6041 (1983); **27**, 1495 (1983); **37**, 2644 (1988); Phase Transit. Crit. Phenom. **12**, 336 (1988).

[68] M. Tokuyama and K. Kawasaki, Phys. Lett. **100A**, 337 (1984); see also Ref. [53(a)]; R. C. Ball and T. A. Witten, Phys. Rev. A **29**, 2966 (1984).

[69] J. F. Douglas, T. Ishinabe, A. M. Nemirovsky, and K. F. Freed, J. Phys. A **26**, 1835 (1993); J. F. Douglas and T. Ishinabe, Phys. Rev. E **51**, 1791 (1995).